

BRIEF REPORTS

Brief Reports are accounts of completed research which do not warrant regular articles or the priority handling given to Rapid Communications; however, the same standards of scientific quality apply. (Addenda are included in Brief Reports.) A Brief Report may be no longer than four printed pages and must be accompanied by an abstract.

Observation of the radiative decay $J/\psi \rightarrow e^+ e^- \gamma$

T. A. Armstrong,⁶ D. Bettoni,² V. Bharadwaj,¹ C. Biino,⁷ G. Borreani,⁷ D. Broemmelsiek,⁵ A. Buzzo,³ R. Calabrese,² A. Ceccucci,⁷ R. Cester,⁷ M. Church,¹ P. Dalpiaz,² P. F. Dalpiaz,² D. Dimitroyannis,⁵ M. Fabbri,² J. Fast,⁴ A. Gianoli,² C. M. Ginsburg,⁵ K. Gollwitzer,⁴ G. Govi,⁷ A. Hahn,¹ M. Hasan,⁶ S. Hsueh,¹ R. Lewis,⁶ E. Luppi,² M. Macri,³ A. M. Majewska,⁶ M. Mandelkern,⁴ F. Marchetto,⁷ M. Marinelli,³ J. Marques,⁵ W. Marsh,¹ M. Martini,² M. Masuzawa,⁵ E. Menichetti,⁷ A. Migliori,⁷ R. Mussa,⁷ S. Palestini,⁷ M. Pallavicini,³ S. Passaggio,³ N. Pastrone,⁷ C. Patrignani,³ J. Peoples, Jr.,¹ F. Petrucci,² M. G. Pia,³ S. Pordes,¹ P. Rapidis,¹ R. Ray,^{5,1} J. Reid,⁶ G. Rinaudo,⁷ B. Rocuzzo,⁷ J. Rosen,⁵ A. Santroni,³ M. Sarmiento,⁵ M. Savriè,² J. Schultz,⁴ K. K. Seth,⁵ A. J. Smith,⁴ G. A. Smith,⁶ M. Sozzi,⁷ S. Trokenheim,⁵ M. F. Weber,⁴ S. Werkema,¹ Y. Zhang,⁶ J. Zhao,⁵ and G. Zioulas⁴
(Fermilab E760 Collaboration)

¹Fermi National Accelerator Laboratory, Batavia, Illinois 60510

²I.N.F.N. and University of Ferrara, 44100 Ferrara, Italy

³I.N.F.N. and University of Genoa, 16146 Genoa, Italy

⁴University of California at Irvine, Irvine, California 92717

⁵Northwestern University, Evanston, Illinois 60208

⁶Pennsylvania State University, University Park, Pennsylvania 16802

⁷I.N.F.N. and University of Turin, 10125 Turin, Italy

(Received 17 July 1996)

We report the first observation of the (radiative) decay $J/\psi \rightarrow e^+ e^- \gamma$. Our data are from an experiment in which J/ψ is formed in antiproton-proton annihilations. The observed rate is consistent with a QED calculation based on final state radiation. Our measurement gives a branching ratio for this mode of $(8.8 \pm 1.3 \pm 0.4) \times 10^{-3}$ for γ energy > 100 MeV. [S0556-2821(96)03223-7]

PACS number(s): 13.75.Cs, 14.40.Gx

The radiative decays $J/\psi \rightarrow e^+ e^- \gamma$ and $J/\psi \rightarrow \mu^+ \mu^- \gamma$ provide a particularly clean test of QED because hadrons are absent in the final state and the radiative decay of the J/ψ to a hadronic state such as a glueball (structural radiation) cannot lead to an $e^+ e^- \gamma$ state to order α . As such they are distinguished from $\rho \rightarrow \pi \pi \gamma$ and $K \rightarrow \pi \pi \gamma$, where structural radiation may be observed. Radiative muon and pion decay, in which the final state is limited to leptons and a γ , are observed to be in agreement with QED at the 20% level [1-3].

The decay $J/\psi \rightarrow e^+ e^- \gamma$ is difficult to study at electron positron colliders. There is interference between the nonresonant $e^+ e^- \rightarrow e^+ e^-$ process (Bhabha scattering) and the process $e^+ e^- \rightarrow J/\psi \rightarrow e^+ e^-$ and γ emission is derived from both initial state and final state electrons. Despite the complication of initial state radiation, the $\mu^+ \mu^- \gamma$ mode was observed by the Mark III experiment [4] at a rate consistent with the prediction of QED final state radiation.

The decay $J/\psi \rightarrow e^+ e^- \gamma$ is described by the diagrams shown in Fig. 1(a) where the γ is emitted by one of the final state electrons. (Radiation of the γ by the J/ψ line, an example of structural radiation, is forbidden by charge-conjugation invariance.) The infrared divergence in the decay rate is canceled by the interference of the diagrams shown in Fig. 1(b) as (was originally) shown by [5]. Follow-

ing the QED formalism of Ref. [6], we adopt the expression for the differential decay rate in the $l^+ l^-$ c.m. frame, which is suitable for finite γ energies:

$$d\Gamma_{J/\psi \rightarrow l^+ l^- \gamma} = d\Gamma_{J/\psi \rightarrow l^+ l^-} \beta'^3 \frac{2\alpha}{\pi} \frac{dE'_\gamma s'}{E'_\gamma s} \times \frac{1 - \cos^2 \theta'_{\gamma l}}{(1 - \beta'^2 \cos^2 \theta'_{\gamma l})^2} d\Omega'_\gamma. \quad (1)$$

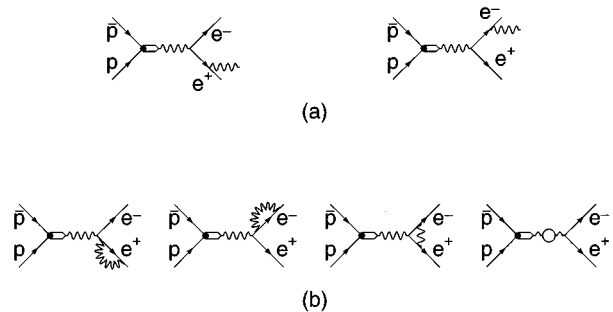


FIG. 1. Diagrams for final state radiation. The decay $J/\psi \rightarrow e^+ e^- \gamma$ is described by (a). The infrared divergence in the decay rate is canceled by interference with the diagrams in (b).

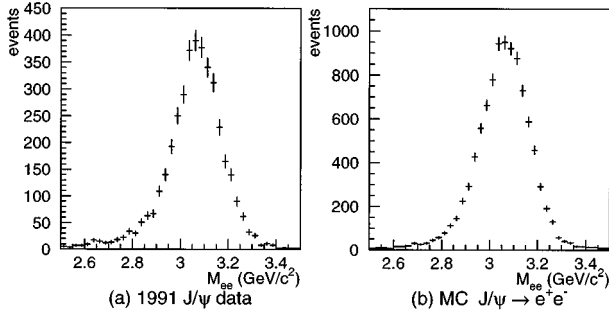


FIG. 2. $M_{e^+e^-}$ for (a) $J/\psi \rightarrow e^+e^-$ candidate events, (b) $J/\psi \rightarrow e^+e^-$ Monte Carlo events.

The differential decay rate for $J/\psi \rightarrow l^+l^-$ in the l^+l^- c.m. frame, which appears in Eq. (1), is given by

$$d\Gamma_{J/\psi \rightarrow l^+l^-} = \frac{3}{3+\lambda} (1 + \lambda \cos^2 \theta'_l) \Gamma_{J/\psi \rightarrow l^+l^-} \frac{d\Omega'_l}{4\pi}. \quad (2)$$

E'_γ represents the γ energy, θ'_γ and ϕ'_γ (Ω'_γ) the γ angles, and θ'_l and ϕ'_l (Ω'_l) the lepton angles, all in the l^+l^- c.m. frame in which the antiproton direction is the polar axis. β' is the lepton velocity and $\theta'_{\gamma l}$ the angle between the lepton and γ directions, also in the l^+l^- c.m. frame. s' is the l^+l^- invariant mass squared and s the J/ψ invariant mass squared. The rate for $J/\psi \rightarrow l^+l^- \gamma$ varies as $1/E'_\gamma$ and has a sharp maximum at an extremely small value of $\theta'_{\gamma l}$.

Experiment E760 is located at the Fermilab Antiproton Source. The circulating antiproton beam in the accumulator ring ($\approx 4 \times 10^{11} \bar{p}$) intersects an internal H_2 gas jet target [$\leq 10^{14}$ (atoms/cm²)], giving a peak luminosity of up to 1.0×10^{31} cm⁻² sec⁻¹. For these data, the luminosity was limited to 4.0×10^{30} cm⁻² sec⁻¹. E760 is devoted to high resolution studies of charmonium formed in antiproton-proton annihilation and is fully described elsewhere [7]. This measurement is based on 661 nb⁻¹ of data taken in 1991 at the formation energy of the J/ψ , in which about 4000 $\bar{p}p \rightarrow J/\psi \rightarrow e^+e^- (X)$ were recorded.

The elements of the E760 detector germane to this measurement are the threshold Čerenkov counter [8] which pro-

vides electron identification and covers the full azimuthal range and a polar angle range from 15° to 70°; the lead glass central calorimeter (CCAL) [9] which covers the full azimuthal range and the polar angle range 11° to 70°; and the radial projection chamber (RPC) [10], which covers the full azimuth and a polar angle range 15° to 70° and provides dE/dx information to distinguish conversion pairs from single electrons.

Two cylindrical plastic scintillator hodoscopes, ($H1$ and $H2$), are used for triggering. The pulse heights in those counters are also used to distinguish singly charged particles from electron positron pairs. For electromagnetic showers of electrons and γ 's, CCAL gives an average resolution of $\sigma_E/E = 0.014 + 0.06/\sqrt{E}$ (GeV) for the energy, 6 mr for σ_θ , and 12 mr for σ_ϕ , where the angular errors include the uncertainty in the annihilation location. CCAL is not instrumented with time-to-digital converters (TDCs). Most showers with energies above 200 MeV can be identified as "in-time" or "out-of-time" by means of a system of analogue-to-digital converters (ADCs) with overlapping gates, described in Ref. [11]. The remainders are identified as "undetermined."

The hardware trigger used to obtain these data required a pattern of hits in the cylindrical hodoscope arrays and the Čerenkov counter consistent with two electrons originating at the beam target intersection point. Additional hodoscope hits were allowed to avoid event loss due to extraneous tracks, mainly δ rays from the target and from interactions of the electrons in the detector materials. The trigger also required two high energy showers in CCAL, separated by at least 90° in azimuth. Each of these showers was required to be loosely consistent with the kinematics of $J/\psi \rightarrow e^+e^-$ decay. This condition accepts events with e^+e^- effective mass greater than about 2.2 GeV/c² with full efficiency.

The hodoscope hits, Čerenkov signals, and calorimeter showers were associated off line into tracks. The two electron candidates were taken as the tracks with the largest two-body effective mass. Since the Čerenkov counter has a region of reduced efficiency in the interval $33^\circ < \theta < 39^\circ$, it was required that the electron candidates be associated with Čerenkov counter hits for all polar angles except those within that interval.

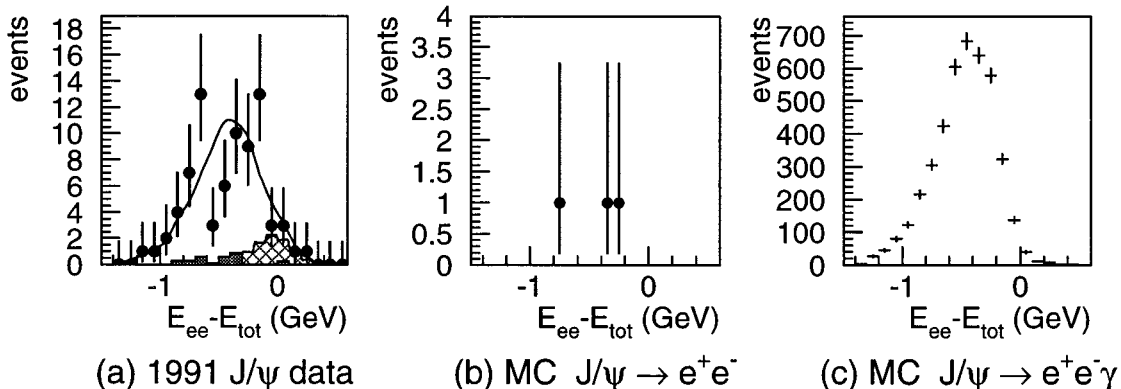


FIG. 3. $E_{ee} - E_{tot}$ for (a) $J/\psi \rightarrow e^+e^-$ candidates which pass the $J/\psi \rightarrow e^+e^- \gamma$ selection. The curve is a fit to $J/\psi \rightarrow e^+e^- \gamma$ plus backgrounds as described in the text. The shaded and cross-hatched histograms are the contributions of nonresonant and accidental backgrounds, respectively, (b) $J/\psi \rightarrow e^+e^-$ Monte Carlo events, and (c) $J/\psi \rightarrow e^+e^- \gamma$ Monte Carlo events.

A sample of 3933 J/ψ candidates was selected using the following cuts: θ_1 and $\theta_2 \in [15^\circ, 60^\circ]$; $M_{e^+e^-} > 2.5$ GeV/ c^2 ; $ELW_1 \times ELW_2 > ELWCUT$. The electron weight index (ELW) is a likelihood ratio for the electron hypothesis versus the background track hypothesis, constructed for each electron candidate from pulse heights in the $H2$ and Cerenkov counters, dE/dx from the RPC, second moments of the transverse shower distribution in CCAL, and the fractional shower energy in a 3×3 block region of CCAL [7]. The cut chosen retains e^+e^- (X) events with 91% efficiency. We observe that this efficiency cancels in the analysis we present below. The e^+e^- mass spectrum for these events is shown in Fig. 2(a).

From the J/ψ candidate events, 77 candidates for $J/\psi \rightarrow e^+e^- \gamma$ were selected by requiring that only one shower accompanying the e^+ and e^- showers pass the following cuts on measured quantities: the extra shower energy > 200 MeV; the extra shower makes an angle with both e^+ and e^- of at least 200 mrad; the extra shower is identified as in-time or undetermined. These requirements remove most external bremsstrahlung events and those $e^+e^- \gamma$ events for which the γ is so close to an electron that the showers merge.

To determine the acceptance of these cuts, we generated 10 000 $\bar{p}p \rightarrow J/\psi \rightarrow e^+e^-$ and 60 000 $\bar{p}p \rightarrow J/\psi \rightarrow e^+e^- \gamma$ events that pass a simulation of the trigger. The distribution in positron angle with respect to the incident antiproton is modeled according to the form (2) with λ determined from our data (Ref. [7]) (0.88 ± 0.19). GEANT [12] was used to track the primary particles through the E760 detector where interactions with materials were simulated. These simulated event sets were subjected to the same analysis as the data, for both the $J/\psi \rightarrow e^+e^-$ and $J/\psi \rightarrow e^+e^- \gamma$ selections. We normalized the simulation to the 3933 J/ψ candidate events observed. Figure 2(b) shows the simulation results for the process $J/\psi \rightarrow e^+e^-$. The agreement between the simulated events and data passing the $J/\psi \rightarrow e^+e^-$ selection, shown in Fig. 2(a), is excellent except for a low mass tail in the data which contains $J/\psi \rightarrow e^+e^- \gamma$ events.

In Fig. 3 we show the distribution in the variable $E_{ee} - E_{tot}$ for the $J/\psi \rightarrow e^+e^- \gamma$ candidates from the data [Fig. 3(a)] and from the two Monte Carlo samples, Figs. 3(b) and 3(c). E_{ee} is the sum of measured energies for the electron candidates and E_{tot} is the total energy. By applying the $e^+e^- \gamma$ selection to the $J/\psi \rightarrow e^+e^-$ Monte Carlo sample, Fig. 3(b), we find that radiation in the detector materials or misreconstruction of electromagnetic showers in CCAL contributes a background of 1.0 ± 0.6 events to the data. The remaining events are therefore due to the radiative decay and other backgrounds. We expect a background due to nonresonant $\bar{p}p$ annihilation, principally $\bar{p}p \rightarrow \pi^0 \pi^0$, in which Dalitz decays and photon conversions lead to events satisfying the selection for $e^+e^- \gamma$. We estimate this background by applying the $e^+e^- \gamma$ selection to data collected in the region of the η_c . After normalizing by integrated luminosity, we obtain an estimate of 3.0 ± 1.0 events, which includes approxi-

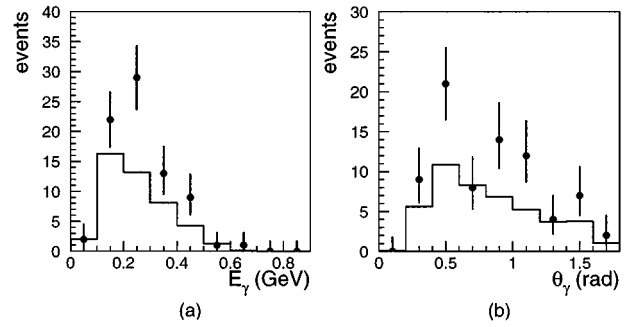


FIG. 4. (a) Energy of γ in J/ψ frame. (b) Angle between γ and nearest electron or positron in J/ψ frame. The histograms (solid line) are predictions of the $e^+e^- \gamma$ simulation.

mately 0.05 nonresonant $e^+e^- \gamma$ events, based on our determination of the direct process $\bar{p}p \rightarrow e^+e^-$ [13]. An additional “accidental” background is from events in which the e^+ and e^- are from a J/ψ decay and the extra cluster is from an unrelated event, close enough in time to count within the ADC gate. Such events produce a peak at zero in the distribution of $E_{ee} - E_{tot}$. We estimate this background by fitting that distribution for the $J/\psi \rightarrow e^+e^- \gamma$ candidates, after subtraction of the nonresonant background, to the sum of the distribution for $J/\psi \rightarrow e^+e^-$ and the distribution for $J/\psi \rightarrow e^+e^- \gamma$, both determined by Monte Carlo simulation. We find that 10.4 ± 5.2 events can be attributed to the accidental background. The best fit is shown with the data and both background contributions in Fig. 3(a).

We show an absolute comparison between our simulation and the data for the γ energy in the J/ψ frame [Fig. 4(a)] and for the angle between the γ and the nearest electron in the J/ψ frame [Fig. 4(b)].

Subtracting all backgrounds, the number of $e^+e^- \gamma$ events within our cuts is 62.6 ± 10.3 to be compared to the QED prediction of 44 events, where the normalization is set by the 3933 $J/\psi \rightarrow e^+e^-$ (X) events observed. The agreement is satisfactory. We therefore use the functional dependence of (1) to estimate the branching ratio $B(J/\psi \rightarrow e^+e^- \gamma, E_\gamma > 100 \text{ MeV})$ divided by the branching ratio $B(J/\psi \rightarrow e^+e^-)$ as 0.147 ± 0.022 , compared to the QED prediction of 0.104.

Normalizing to the Particle Data Group [14] value for the branching ratio $B(J/\psi \rightarrow e^+e^-) = (5.99 \pm 0.25) \times 10^{-2}$ we determine the branching ratio $B(J/\psi \rightarrow e^+e^- \gamma, E_\gamma > 100 \text{ MeV})$ to be $(8.8 \pm 1.3 \pm 0.4) \times 10^{-3}$.

The authors wish to acknowledge the help of the members of the Fermilab Accelerator division. We also wish to thank the staff, engineers, and technicians at our respective institutions for their help and cooperation. This research was supported by the U.S. Department of Energy, the U.S. National Science Foundation, and the Istituto Nazionale di Fisica Nucleare of Italy.

- [1] C. Castagnoli and M. Muchnik, *Phys. Rev.* **112**, 1779 (1958).
- [2] V. N. Bolotov *et al.*, *Phys. Lett. B* **265**, 308 (1990).
- [3] R. R. Crittenden and W. D. Walker, *Phys. Rev.* **121**, 1823 (1961).
- [4] J. S. Brown, Ph.D. thesis, University of Washington, 1984.
- [5] F. Bloch and A. Nordsieck, *Phys. Rev.* **52**, 54 (1937).
- [6] J. M. Jauch and F. Rohrlich, *Theory of Photons and Electrons*, 2nd ed. (Springer-Verlag, Berlin, 1976).
- [7] T. Armstrong *et al.*, *Phys. Rev. D* **47**, 772 (1993).
- [8] C. Biino *et al.*, *Nucl. Instrum. Methods Phys. Res. A* **317**, 135 (1992).
- [9] L. Bartoszek *et al.*, *Nucl. Instrum. Methods Phys. Res. A* **301**, 47 (1989).
- [10] R. Calabrese *et al.*, *Nucl. Instrum. Methods Phys. Res. A* **277**, 116 (1989).
- [11] K. E. Gollwitzer, Ph.D. thesis, University of California, Irvine, 1993.
- [12] *GEANT Detector Description and Simulation Tool*, CERN Program Library Long Writeup W5013, 1994.
- [13] T. Armstrong *et al.*, *Phys. Rev. Lett.* **70**, 1212 (1993).
- [14] Particle Data Group, L. Montanet *et al.*, *Phys. Rev. D* **50**, 1173 (1994).